Comparing Polar Lows in Atmospheric Reanalyses: Arctic System Reanalysis versus ERA-Interim

JULIA SMIRNOVA AND PAVEL GOLUBKIN

Satellite Oceanography Laboratory, Russian State Hydrometeorological University, St. Petersburg, Russia

(Manuscript received 29 August 2016, in final form 7 March 2017)

ABSTRACT

Representation of polar lows in the new high-resolution Arctic System Reanalysis (ASR) was for the first time assessed and compared to that in the ERA-Interim. Substantial improvements were found in the 850-hPa relative vorticity and near-surface wind speed information. The latter was found to be in close agreement with satellite-derived estimates. Representation of polar lows from a widely used selective list in ERA-Interim and ASR was estimated as 48% and 89%, respectively. The proportion of polar lows represented in ASR is substantially higher than reported for other reanalyses in previous studies. Verifications were found to be sensitive to the polar low reference list used, and to the definition of a polar low. As found, when a more complete polar low list from a recent satellite-derived climatology was used, the proportion of represented events decreased to 26% and 66% for ERA-Interim and ASR, respectively. Variations in polar low representation in reanalyses were also observed in different regions, with the highest proportion resolved in the Norwegian Sea. Strong dependence between polar low sizes and their representation in ERA-Interim was found. In the case of ASR, polar low representation remains constant in the size range of 200–500 km and slightly decreases only for the smallest systems with diameters less than 200 km. Usage of the strict threshold of 43 K for the atmospheric static stability criterion was found to exclude a considerable number of otherwise well-represented polar lows.

1. Introduction

The most intense subclass of polar maritime mesoscale cyclones characterized by horizontal scales less than 1000 km and near-surface wind speeds near or above gale force are the polar lows (PLs), which are found on both hemispheres and form poleward of the main baroclinic zone (Rasmussen and Turner 2003). These cold-season phenomena have a lifetime that is generally only 12–36 h (Blechschmidt 2008; Smirnova et al. 2015), which in conjunction with their small size and a relatively sparse in situ network in polar regions severely limits their identification on weather maps and forecasting by numerical models. In the past, this sometimes led to complete mariners' and coastal communities' unawareness of the danger they might encounter, which includes icing, high waves, strong winds, and heavy snowfall. Indeed, reports of shipwrecks along with weather maps and a few satellite infrared images were even used for the first climatology of PLs in the Norwegian Sea (Wilhelmsen 1985). Further climatologies are mainly focused on the Nordic seas (i.e., Norwegian, Barents, and Greenland Seas) and build on an increased availability of satellite data in the following decades (Blechschmidt 2008; Noer et al. 2011; Smirnova et al. 2015) or on an improved ability of numerical models to reproduce such unique events (e.g., Bracegirdle and Gray 2008; Zahn and von Storch 2008) using global atmospheric reanalyses data as initial and boundary conditions.

However, representation of these phenomena in the reanalyses themselves is of concern. Recently, Laffineur et al. (2014) analyzed 29 PLs spanning three seasons (1999/2000–2001/02) and found that approximately 24% and 45% of them are represented in the mean sea level pressure (MSLP) fields from the 40-yr European Centre for Medium-Range Weather Forecasts (ECMWF) Re-Analysis (ERA-40) and ERA-Interim, respectively. The reanalyses data were then dynamically downscaled with a higher-resolution (12 km) mesoscale model Meso-NH. This allowed more cases to appear in simulations and resulted in an improved representation of PLs (61% and 79% using the ERA-40 and ERA-Interim

Corresponding author e-mail: Julia Smirnova, jsmirnova@rshu.ru

DOI: 10.1175/MWR-D-16-0333.1

data, respectively). Similarly, Zappa et al. (2014) used the 850-hPa relative vorticity, near-surface wind speed, and atmospheric static stability criteria to track PLs with an automated procedure. They found that about 55% and 70% of PLs are represented in ERA-Interim and ECMWF operational analysis, respectively, when examining 34 cases between 2008/09 and 2010/11 seasons.

As such, representation of PLs in reanalysis datasets remains insufficient, though considerable progress was made in the recent years tied to improvements of reanalyses including enhanced horizontal and vertical resolutions, improved physical schemes, and advances in data assimilation methods. In that context, emergence of the Arctic System Reanalysis (ASR; Bromwich et al. 2010), which was already shown to better resolve other mesoscale phenomena (Moore et al. 2015), as well as synoptic-scale cyclones (Tilinina et al. 2014), allows us to expect further improvements concerning representation of PLs. Indeed, the effective resolution of ASR was found to be 150 km (Moore et al. 2015), which may be sufficient to resolve PLs characterized by an average size of 300 km (Blechschmidt 2008; Smirnova et al. 2015). This is in contrast to ERA-Interim, which has the effective resolution of 400 km (Moore et al. 2015), and is not able to resolve a substantial part of observed PLs (Laffineur et al. 2014; Zappa et al. 2014).

On the other hand, the existing estimates of PL representation in reanalyses might have been influenced by a limited number of cases that PL lists used as a reference contain. For example, both Laffineur et al. (2014) and Zappa et al. (2014) derived such lists from the Noer et al. (2011) climatology, which employed stricter criteria for PL selection and recorded only the most intense event in an outbreak of several PLs. This resulted in a considerably lower number of listed cases (about 12 per year) compared to other studies (Blechschmidt 2008; Bracegirdle and Gray 2008; Zahn and von Storch 2008; Smirnova et al. 2015). Interestingly, 49 extra PLs absent from the reference PL list were found by Zappa et al. (2014) when applying an automated tracking procedure. This implies that the more accurate estimates can be obtained with a more complete reference list. In that context, the recent climatological study by Smirnova et al. (2015), which, as well as the Blechschmidt (2008) 2-yr climatology, is consistent with the widely used PL definition proposed by Rasmussen and Turner (2003), yet contains PL cases for 14 seasons with an annual mean of 45.5 cases, provides an excellent alternative reference list for assessment of PL representation in reanalyses data.

Another aspect that may also influence the results of such assessments is how the decision about representation of a specific PL is made. Recent studies introduced an atmospheric static stability criterion, which is indicative of cold air outbreaks (i.e., a favorable condition for PL development). As such, the temperature difference between the sea surface and air at 500 hPa was required to exceed 43 K in reanalyses (Zappa et al. 2014; Yanase et al. 2016) or other model (Zahn and von Storch 2008) data. However, the relevance of this criterion is uncertain. For example, recently Terpstra et al. (2016) found that its application might exclude forward shear PLs, which generally form in an environment with lower temperature difference.

In this study, representation of PLs in the two reanalysis datasets (i.e., ASR and ERA-Interim), is thus assessed using two reference PL lists—one being a subset of the widely used Noer et al. (2011) climatology and another of the more complete Smirnova et al. (2015) climatology—and the possible impact of the atmospheric static stability criterion on the results is examined.

2. Data and methods

a. *Reanalysis datasets*

ERA-Interim is a global atmospheric reanalysis produced by ECMWF for 1979 onward based on its Integrated Forecast System (IFS) operational spectral model. The data assimilation system uses a 4D variational data assimilation scheme with 12-hourly analysis cycles. The analysis is performed on 60 vertical levels up to 0.1 hPa with 12 levels below 850 hPa. The ERA-Interim has T255 spectral resolution (corresponds to ~79-km horizontal resolution). The data are available every 6 h on a regular 0.75° × 0.75° grid. For more information on ERA-Interim see Dee et al. (2011).

The ASR reanalysis is produced by the Polar Meteorology Group at Byrd Polar and Climate Research Center at The Ohio State University. It is based on the Polar Weather Research and Forecasting (Polar WRF) Model, which is a version of the WRF Model with adaptations relevant for polar regions (i.e., improved boundary layer parameterization and representation of heat transfer, more advanced snow surface and cloud physics, and better sea ice treatment) (Hines and Bromwich 2008; Bromwich et al. 2009). Simulations are performed on 71 vertical levels up to 10 hPa with 25 levels below 850 hPa. Above 100 hPa, Polar WRF is spectrally nudged toward the ERA-Interim state. The ERA-Interim data are also used as initial and lateral boundary conditions. The ASR reanalysis uses a 3D data assimilation scheme with 3-hourly analysis cycles, which assimilates a larger amount of observations in the Arctic and more detailed descriptions of surface

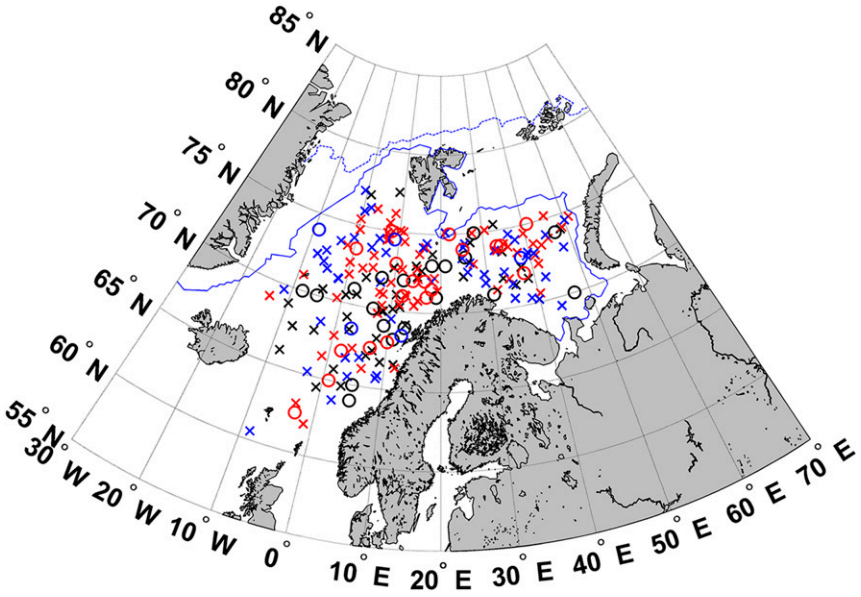

FIG. 1. Spatial distribution of polar lows from subsets of N11 (circles; 46 cases) and S15 (crisscrosses; 158 cases) climatologies used as the two reference lists in the present study. Black symbols correspond to events represented in both reanalyses. Blue symbols correspond to polar lows not represented in both reanalyses. Red symbols correspond to polar lows represented in ASR, but not represented in ERA-Interim. Blue lines show the median (solid line) and 95th percentile (dashed line) of the sea ice extent for the study period. Locations of polar lows correspond to their mature stage (maximum intensity).

conditions. The ASR version 1 (hereafter referred to as ASR) output used here is provided on a staggered Arakawa C grid with 30-km horizontal resolution. The data are available every 3 h from 2000 to 2012. For more information on ASR see Bromwich et al. (2016).

b. *Polar low lists*

The Noer et al. (2011) PL climatology for the Nordic seas (hereafter N11) is mainly based on visual inspection of satellite infrared data from the Advanced Very High Resolution Radiometer (AVHRR; Cracknell 1997). Though wind speed scatterometer data were used in addition to the AVHRR images, a wind speed criterion was not always followed in the selection of cases. Instead, conditions favorable for PL development were required to be present in the HIRLAM model data. If PLs formed in pairs or in a cluster of low pressure systems, only the most intense event was recorded. Overall, the climatology contains 121 cases in 10 years (2000–09).

The Smirnova et al. (2015) satellite climatology (hereafter S15) is also focused on the Nordic seas and is based on manual analysis of passive microwave data from the Special Sensor Microwave Imager (SSM/I; Hollinger et al. 1990). Total atmospheric water vapor content fields retrieved using an algorithm specially designed for Arctic conditions (Bobylev et al. 2010) were visually analyzed to identify mesoscale cyclonic vortices. Then, a wind speed criterion was applied with a threshold of $15\,\mathrm{m\,s^{-1}}$. Accounting for the standard error of the algorithm used for wind speed retrievals ($\sim 0.9\,\mathrm{m\,s^{-1}}$; Wentz 1997), the presence of a group of pixels exceeding the threshold was required. The climatology is consistent with the PL definition proposed by Rasmussen and Turner (2003) and yields 637 cases over 14 seasons (1995/96–2008/09).

In this study two subsets of these climatologies for four consecutive cold seasons (i.e., September–April) from 2000/01 to 2003/04 are used. The resulting reference PL lists contain 46 and 158 cases from the N11 and S15 climatologies, respectively (Fig. 1). Merging of these two reference lists results in 181 unique PL events (hereafter combined reference list).

c. *Identification criteria*

Representation of PLs from the reference lists in the ERA-Interim and ASR data was assessed using a set of criteria. The initial criterion was the relative vorticity intensity at 850 hPa. A T40-T100 bandpass filter was used to filter out large systems and small-scale noise from the relative vorticity data prior to application of the criterion. Such filtering focuses on the spatial scales around 200–500 km (see Laprise 1992). Possible Gibbs

TABLE 1. Number and percentage of polar lows from the reference lists from N11 (46 cases) and S15 (158 cases) that fulfilled the requirements given in column 1 in the ERA-Interim (ERA-I) and ASR data. The listed requirements include criteria on the magnitude of the filtered 850-hPa relative vorticity (RV), near-surface wind speed (Wind), and temperature difference between the sea surface and air at 500 hPa (SST-T500), the combination of two criteria on the magnitude of the filtered 850-hPa relative vorticity and near-surface wind speed (RV+Wind), and the combination of all three criteria.

	N11 (46)				S15 (158)			
	ERA-I		ASR		ERA-I		ASR	
RV	27	58.7%	43	93.5%	80	50.6%	134	84.8%
Wind	31	67.4%	44	95.7%	66	41.8%	144	91.1%
SST-T500	45	97.8%	45	97.8%	129	81.6%	130	82.3%
RV+Wind	23	50.0%	42	91.3%	49	31.0%	126	79.7%
All three criteria	22	47.8%	41	89.1%	41	25.9%	104	65.8%

oscillations caused by this procedure were reduced by applying the spectral taper described in Sardeshmukh and Hoskins [1984, their Eq. (9)]. PLs in the reanalyses data were required to have a maximum larger than $6 \times 10^{-5}\,s^{-1}$ in the T40-T100 filtered 850-hPa relative vorticity fields. According to the Rasmussen and Turner (2003) definition, PLs produce winds of near gale force or above. As such, the near-surface wind speed was required to be higher than $15\,m\,s^{-1}$. An atmospheric stability criterion indicative of cold air outbreaks was also introduced. The difference between the sea surface temperature and the air temperature at 500 hPa (SST-T500) was thus required to be larger than 43 K. Overall, the described set of criteria corresponds to the one used by Zappa et al. (2014).

Fulfillment of the criteria in the reanalyses data was manually checked after plotting the corresponding parameters and overlaying PL tracks (for the list from S15) or locations where PLs reached their mature stage (for the list from N11). When necessary, the AVHRR data were used to reconstruct tracks for PLs from N11. No automated procedures for PL tracking were invoked and no additional PLs were sought except those listed in the reference lists. We believe that the manual analysis allowed us to best eliminate possible discrepancies caused by the different number of track points in the reference lists and different temporal resolution of reanalyses. However, the latter might be of concern for the shortest-lived PLs with lifetimes less than 6 h. Nevertheless, they account for only less than 3% of the total number of PLs (Smirnova et al. 2015) and their impact on results is considered to be negligible in the present study.

3. Results

The overall results described below are summarized in Table 1. First, the ERA-Interim data were analyzed to find signatures of PLs from N11 using the abovementioned set of criteria. Maxima in the filtered 850-hPa relative vorticity above $6 \times 10^{-5}\,s^{-1}$ were found in 58.7% of cases. For the wind speed, 67.4% of cases fulfilled the $15\,m\,s^{-1}$ criterion. In all but one case, ERA-Interim indicated unstable atmospheric conditions with SST-T500 difference of more than 43 K. Upon combining the three criteria, 47.8% of PLs from N11 are represented in ERA-Interim. This approximately corresponds to Zappa et al. (2014) and Laffineur et al. (2014) where smaller subsets of the same PL climatology were utilized. When the reference PL list from S15 was used, the representation was found to be much lower. Out of 158 cases composing the list, 50.6% fulfilled the relative vorticity criterion, in 41.8% of cases the maximum wind speed values reached at least $15\,m\,s^{-1}$, and the favorable SST-T500 difference was found in 81.6% of cases. Overall representation was estimated as 25.9%.

Similarly, representation of PLs from N11 was assessed using ASR data. Striking improvements were observed in the 850-hPa relative vorticity intensity, with 93.5% of cases exceeding the threshold. Significant enhancement of wind speeds in PL situations was also noted in ASR, which indicated values greater than $15\,m\,s^{-1}$ in all but two cases (95.7%). Figure 2 illustrates a typical case when, unlike ERA-Interim, ASR is able to reproduce high values of both 850-hPa relative vorticity and wind speed found within a PL. No improvements in the SST-T500 parameter were found and the absence of high atmospheric instability, which was indicated for one case by ERA-Interim, was indicated by ASR as well. Enhancements of the relative vorticity and wind speed parameters introduced in ASR are therefore attributed for almost doubling the proportion of PLs represented in ERA-Interim, which for ASR was estimated as 89.1%. These improvements are even more pronounced when the reference list from S15 is used. Using ASR data, 84.8% and 91.1% of cases fulfilled the relative vorticity and wind speed criteria, respectively. For one more case, the

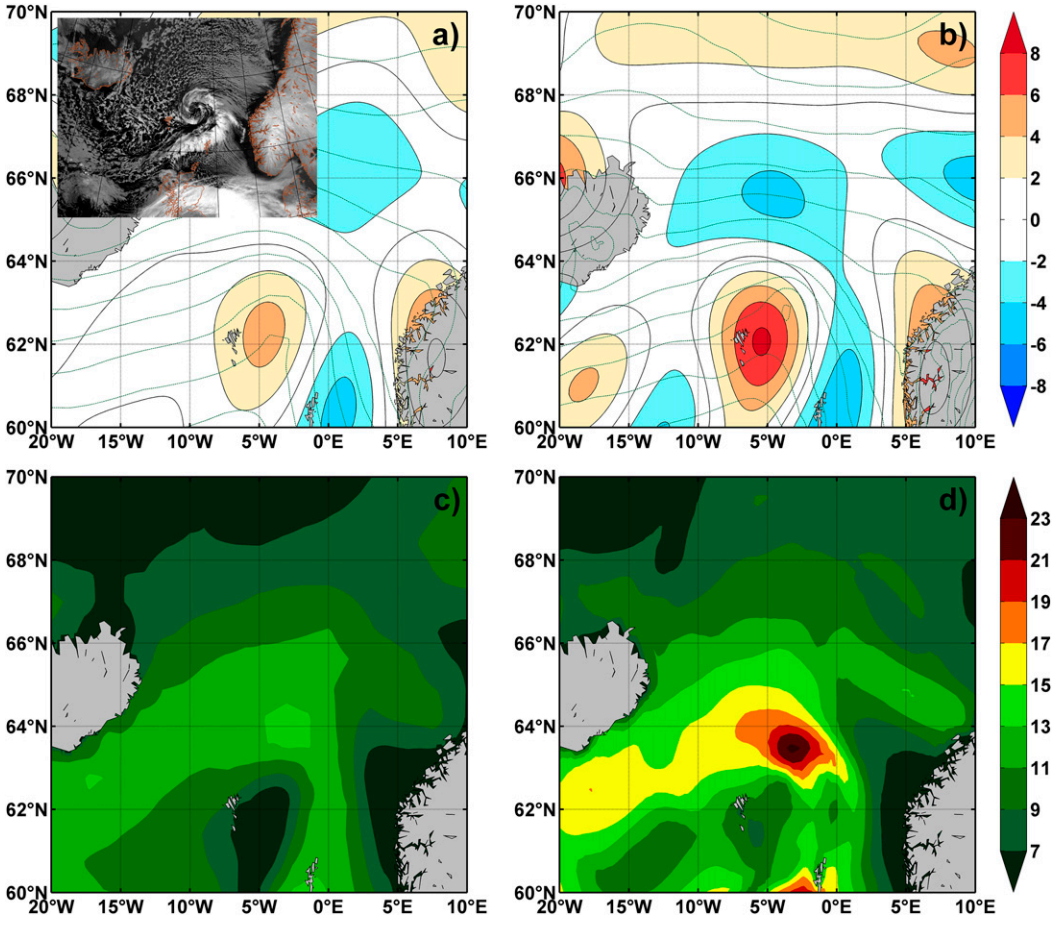

FIG. 2. Reanalysis data for a polar low centered approximately at 62.5°N, 3°W at 1800 UTC 4 Feb 2001. (top) T40-T100 filtered 850-hPa relative vorticity (10^{-5} s^{-1}) fields (shaded; solid black lines) and MSLP contours (dashed green lines) from (a) ERA-Interim and (b) ASR. (bottom) Near-surface wind speed (m s^{-1}) fields from (c) ERA-Interim and (d) ASR. (top left) The AVHRR infrared image for 1612 UTC indicates the location of the polar low.

SST-T500 difference was found to be larger than 43 K. Overall, 104 out of 158 cases passed all three criteria, or approximately 66%. This proportion is 2.5 times larger than estimated using ERA-Interim data, although, again, considerably smaller than when the reference list from N11 was used.

Analyzing spatial distribution of PLs (Fig. 1) one may note certain variations in proportion of PLs resolved by reanalyses in different regions. The combined reference list (see section 2b) was used to assess PL representation separately for the Norwegian, Barents, and Greenland Seas (Table 2). As found, the representation in both reanalyses is highest in the Norwegian Sea. Furthermore, PL representation in ASR is almost equal in the Barents and Greenland Seas, whereas ERA-Interim resolves a considerably lower fraction of PLs in the Greenland Sea. Such regional variations may be attributed to differences in the number of assimilated observations and in sea ice coverage. One may also note a cluster of PLs located approximately at 75°N, 10°E (Fig. 1), which is represented only in ASR. This location is typical for boundary layer–front-type PLs that develop when minor vortices that originate close to the sea ice edge along a front separating relatively warm maritime air masses and colder air masses over sea ice and snow are intensified by upper-level forcing (Rasmussen and Turner 2003). As such, improved

TABLE 2. Number and percentage of polar lows from the combined reference list represented in the ERA-Interim (ERA-I) and ASR data.

	ERA-I		ASR		Total
Norwegian Sea	37	38.1%	78	80.4%	97
Barents Sea	13	22.4%	33	56.9%	58
Greenland Sea	2	7.7%	14	53.8%	26

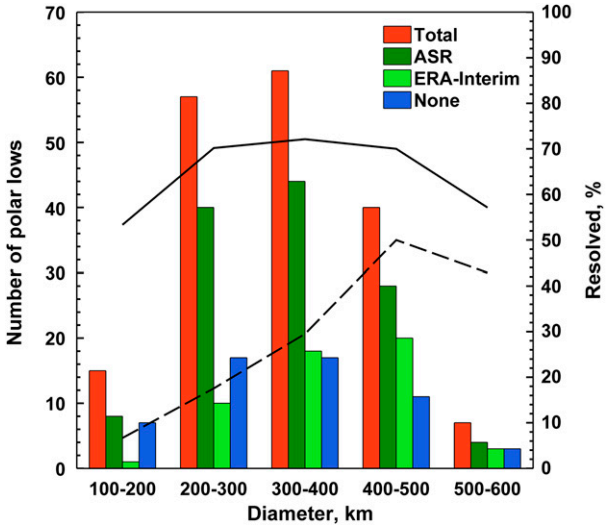

FIG. 3. Size distribution of polar lows from the combined reference list and their representation in reanalyses. Bars (left axis) correspond to the total number of polar lows (red), the number of polar lows represented in ASR (dark green), ERA-Interim (light green), and not represented in both reanalyses (blue). Lines (right axis) show proportion of polar lows resolved by ASR (solid line) and ERA-Interim (dashed line).

boundary layer parameterization and better sea ice treatment implemented in Polar WRF allowed ASR to capture such developments.

Relation between PL sizes and their representation in reanalyses was also examined (Fig. 3). For this purpose, diameters of all PLs from the combined reference list were estimated in the same manner as in Smirnova et al. (2015). As found, the performance of ERA-Interim gradually improves with increasing PL size from 6.6% for systems with diameters of 100–200 km to 50% for larger PLs with 400–500-km sizes. Such dependence was not noted for ASR whose performance remains almost constant in the size range of 200–500 km with approximately 70% of PLs resolved. This proportion decreases only for the smallest systems with horizontal extents of 100–200 km with 53% of such PLs reproduced. For PLs with 500–600-km diameters, representation in both reanalyses decreases, but this is apparently only due to a very limited sample size since only seven cases fell into this category. The present results for ERA-Interim are in line with Condron et al. (2006) where strong dependence between diameters of polar mesocyclones and probability of them having a signature in ERA-40 MSLP fields was observed. For PLs, however, Laffineur et al. (2014) found no relation between sizes and representation in ERA-40 and ERA-Interim after analysis of 29 cases. Presumably, insufficient sample size might have influenced their results as it did ours for the small group of largest systems with diameters of more than 500 km.

The maximum wind speed values found within PLs from the combined reference list in reanalyses data were further examined and compared with the ones derived from the SSM/I satellite microwave radiometer measurements for corresponding events (Fig. 4). The SSM/I wind speed product provided by the Remote Sensing Systems on a $0.25° \times 0.25°$ grid was used for this comparison. As found, the wind speeds recorded in ASR are in reasonable agreement with the satellite-derived estimates while the ERA-Interim values are considerably lower. Correspondingly, the root-mean-square and mean absolute errors are lower for ASR than for ERA-Interim, while the correlation coefficient is higher and the slope of the least squares fit is closer to unity. The mean percentage increase in the wind speed magnitude from ERA-Interim to ASR was estimated as 32.3%.

Comparing the two reanalyses, no notable differences were found in the SST-T500 parameter. This may be due to assimilation of the ERA-Interim sea surface temperatures in ASR (Bromwich et al. 2016) and very little variation of the air temperature at 500 hPa present on scales below those resolved by ERA-Interim. As for the impact of this criterion on estimation of PL representation, it was found to be negligible for the list from N11 where only in one case the threshold of 43 K is not reached. However, considerable effect of this criterion was observed for the list from S15 in which about 18% of cases exhibit values less than this threshold. Values of the SST-T500 parameter for PLs from this list lay between 36 and 55 K with a mean value of 46 K (Fig. 5). Similar values (34–54 K) were found by Blechschmidt et al. (2009) for the 2-yr PL climatology also consistent with the Rasmussen and Turner (2003) PL definition (Blechschmidt 2008). Recently, Terpstra et al. (2016) analyzed 131 PLs from a dataset based on the N11 climatology and reported that values of the SST-T500 parameter were in 33–53-K range. Moreover, it was found that during forward shear PLs, which constituted about 19% of the analyzed dataset, the threshold of 43 K is generally not exceeded. As such, the atmospheric static stability criterion with 43-K threshold discards otherwise well-represented PLs. Without this criterion, the resulting representation of PLs from S15 would grow to about 31% and 80% for ERA-Interim and ASR, respectively. Same results would be obtained if the threshold was decreased to 36 K, since no PLs from the reference lists have lower values of the SST-T500 parameter in the reanalyses data.

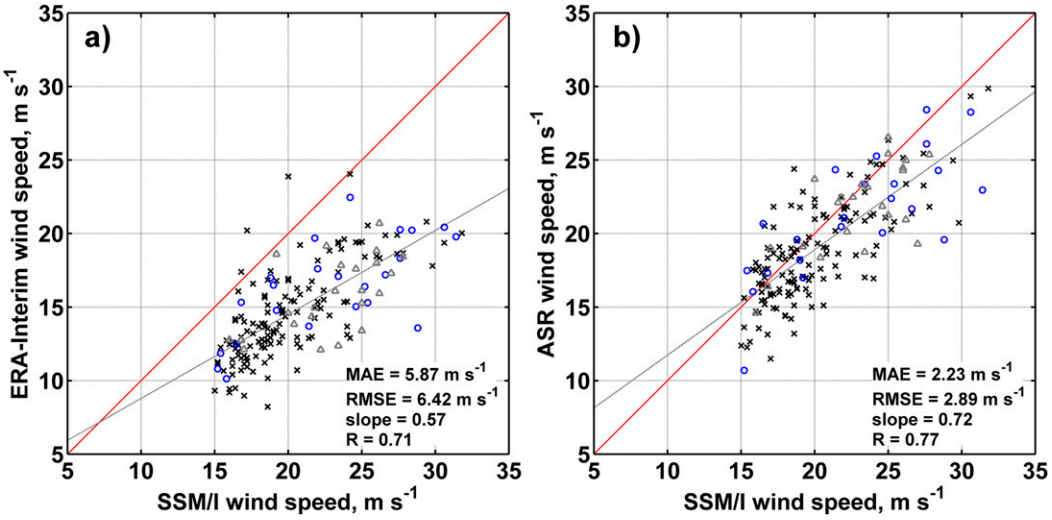

FIG. 4. Scatterplot of maximum wind speed values found within polar lows in (a) ERA-Interim and (b) ASR data vs SSM/I satellite passive microwave instrument estimates. Blue (black) symbols correspond to polar lows that are unique to N11 (S15) climatology. Gray symbols correspond to polar lows common to both N11 and S15 climatologies. Statistical parameters (mean absolute and root-mean-square errors, slope of the least squares fit, and correlation coefficient) for the combined reference list are given in the bottom-right corner of each plot. Gray dashed lines represent linear regressions. One-to-one relations are shown as red lines.

4. Discussion and conclusions

Representation of PLs in the new high-resolution reanalysis focused on the Arctic region was for the first time assessed and compared to that of the ERA-Interim reanalysis. Substantial improvements were found, confirming the ability of ASR to better resolve mesoscale features. As found, the 850-hPa relative vorticity in PLs is more intense in ASR compared to ERA-Interim. The amount of PLs fulfilling this criterion drastically increased for both PL lists. As analyzed, the ASR wind speed information is also more realistic in PL situations and is in closer agreement with the satellite-derived estimates. Overall, approximately 48% of PLs from N11 were found in ERA-Interim. For ASR this percentage was estimated as 89%. Recent studies, which used different subsets of the same N11 climatology, indicated that PLs are best represented in the ECMWF operational analysis data [representation was estimated as 70% by Zappa et al. (2014)] and in simulations of a mesoscale model with the ERA-Interim data used as initial conditions [79% of PLs were found by Laffineur et al. (2014)]. As such, the ability of ASR to reproduce PLs was found to be substantially superior to these estimates. Note that the mesoscale model used by Laffineur et al. (2014) had 12-km spatial resolution [i.e., higher than the spatial resolution of ASR data used here (30 km)]. This suggests that higher resolution does not always lead to better resolving of PLs and is not the only reason of the improved PL representation in reanalyses. In the case of ASR the improvements may be attributed to the use of the Polar WRF Model, which was carefully tuned for the Arctic conditions, and the larger amount of assimilated data.

As found, the choice of the reference PL list used in such estimations may indeed influence the results. When the list from S15 which contains 3.5 times more cases

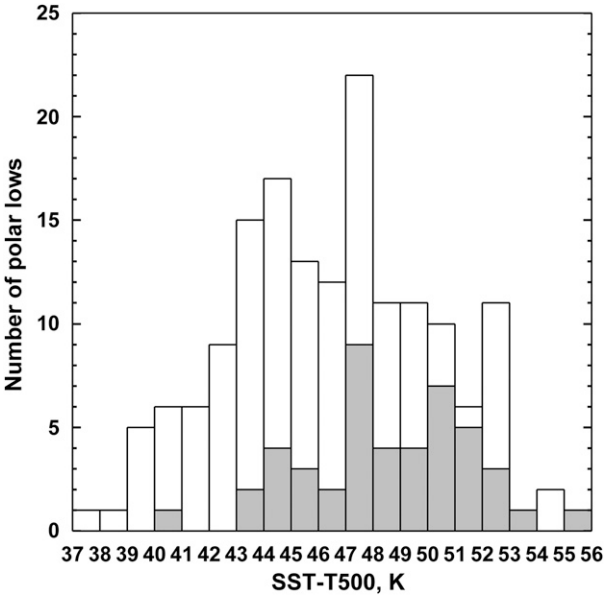

FIG. 5. Maximum values of the SST-T500 difference in the ASR data for polar lows from the reference lists from N11 (gray bars) and S15 (white bars).

than the one from N11 over the same time period is used, the proportion of represented PLs notably decreases. As estimated, only in 26% and 66% of cases all three criteria are fulfilled in the ERA-Interim and ASR data, respectively. This difference may be attributed to the nature of these lists. While the S15 satellite climatology was compiled in accordance with the conventional Rasmussen and Turner (2003) PL definition, which includes requirements on diameter, lifetime, and wind speed, the selection of events for the N11 climatology was performed more subjectively and was down to forecasters' judgment after identification of a PL on satellite infrared imagery and following an analysis of its development using model data.

As analyzed, PL representation in reanalyses is uneven in different regions. For both reanalyses, it is highest in the Norwegian Sea. Approximately equal proportions of PLs are resolved by ASR in the Barents and Greenland Seas, whereas ERA-Interim resolves a much lower fraction of PLs in the latter. Furthermore, a strong dependence between PL sizes and their representation in ERA-Interim was found. In the case of ASR, PL representation is slightly lower only for the smallest vortices with diameters less than 200 km and remains constant for the rest of the systems.

As analyzed, usage of the strict threshold of 43 K for the SST-T500 parameter in studies concerned with representation of PLs in reanalyses or utilizing automated tracking procedures to track the events leads to exclusion of a considerable number of PLs. This is in agreement with Terpstra et al. (2016) where forward shear PLs were shown to generally form in an environment with the SST-T500 values less than 43 K. As found, no PLs from the reference lists have values less than 37 K in the ASR data or less than 36 K in the ERA-Interim data (with only one less than 37 K). This means that 37 K, or possibly 36 K, might be a better threshold value, since it would not exclude the otherwise resolved PLs. Future studies are certainly required to examine the relevance of the SST-T500 parameter for automated tracking procedures and influence of altering the threshold on correct selection of maximum possible number of events along with minimizing number of false positive ones.

Acknowledgments. The authors wish to thank the anonymous reviewers for their constructive comments and suggestions that led to substantial improvements to the manuscript. The authors are grateful to ECMWF for the ERA-Interim data (available online at http://apps.ecmwf.int/datasets/data/interim-full-daily/). We are also grateful to the Polar Meteorology Group at Byrd Polar and Climate Research Center, The Ohio State University, for production of ASR (data are available online at http://rda.ucar.edu/datasets/ds631.0/). The authors are thankful to NERC Satellite Receiving Station, Dundee University, Scotland, for AVHRR data (http://www.sat.dundee.ac.uk/). PL cases from N11 used in this study are available in Noer and Lien (2010). PL cases from S15 used in this study are available at doi:10.17632/ggbt77tfk6.2. This study was supported by Russian Foundation for Basic Research Grant 16-35-00504 and Russian Ministry of Education and Science Project 5.2928.2017/PP.

REFERENCES

Blechschmidt, A.-M., 2008: A 2-year climatology of polar low events over the Nordic seas from satellite remote sensing. *Geophys. Res. Lett.*, **35**, L09815, doi:10.1029/2008GL033706.

——, S. Bakan, and H. Graßl, 2009: Large-scale atmospheric circulation patterns during polar low events over the Nordic seas. *J. Geophys. Res.*, **114**, D06115, doi:10.1029/2008JD010865.

Bobylev, L. P., E. V. Zabolotskikh, L. M. Mitnik, and M. L. Mitnik, 2010: Atmospheric water vapor and cloud liquid water retrieval over the Arctic Ocean using satellite passive microwave sensing. *IEEE Trans. Geosci. Remote Sens.*, **48**, 283–294, doi:10.1109/TGRS.2009.2028018.

Bracegirdle, T. J., and S. L. Gray, 2008: An objective climatology of the dynamical forcing of polar lows in the Nordic seas. *Int. J. Climatol.*, **28**, 1903–1919, doi:10.1002/joc.1686.

Bromwich, D. H., K. M. Hines, and L. S. Bai, 2009: Development and testing of polar Weather Research and Forecasting Model: 2. Arctic Ocean. *J. Geophys. Res.*, **114**, D08122, doi:10.1029/2008JD010300.

——, Y. H. Kuo, M. Serreze, J. Walsh, L.-S. Bai, M. Barlage, K. Hines, and A. Slater, 2010: Arctic system reanalysis: Call for community involvement. *Eos, Trans. Amer. Geophys. Union*, **91**, 13–14, doi:10.1029/2010EO020001.

——, A. B. Wilson, L. S. Bai, G. W. Moore, and P. Bauer, 2016: A comparison of the regional Arctic System Reanalysis and the global ERA-Interim Reanalysis for the Arctic. *Quart. J. Roy. Meteor. Soc.*, **142**, 644–658, doi:10.1002/qj.2527.

Condron, A., G. R. Bigg, and I. A. Renfrew, 2006: Polar mesoscale cyclones in the northeast Atlantic: Comparing climatologies from ERA-40 and satellite imagery. *Mon. Wea. Rev.*, **134**, 1518–1533, doi:10.1175/MWR3136.1.

Cracknell, A. P., 1997: *Advanced Very High Resolution Radiometer AVHRR*. CRC Press, 968 pp.

Dee, D. P., and Coauthors, 2011: The ERA-Interim reanalysis: Configuration and performance of the data assimilation system. *Quart. J. Roy. Meteor. Soc.*, **137**, 553–597, doi:10.1002/qj.828.

Hines, K. M., and D. H. Bromwich, 2008: Development and testing of Polar WRF. Part I: Greenland ice sheet meteorology. *Mon. Wea. Rev.*, **136**, 1971–1989, doi:10.1175/2007MWR2112.1.

Hollinger, J. P., J. L. Peirce, and G. A. Poe, 1990: SSM/I instrument evaluation. *IEEE Trans. Geosci. Remote Sens.*, **28**, 781–790, doi:10.1109/36.58964.

Laffineur, T., C. Claud, J.-P. Chaboureau, and G. Noer, 2014: Polar lows over the Nordic Seas: Improved representation in ERA-Interim compared to ERA-40 and the impact on downscaled simulations. *Mon. Wea. Rev.*, **142**, 2271–2289, doi:10.1175/MWR-D-13-00171.1.

Laprise, R., 1992: The resolution of global spectral models. *Bull. Amer. Meteor. Soc.*, **73**, 1453–1454.

Moore, G. W. K., I. A. Renfrew, B. E. Harden, and S. H. Nernild, 2015: The impact of resolution on the representation of southeast Greenland barrier winds and katabatic flows. *Geophys. Res. Lett.*, **42**, 3011–3018, doi:10.1002/2015GL063550.

Noer, G., and T. Lien, 2010: Dates and positions of Polar Lows over the Nordic Seas between 2000 and 2010. Norwegian Meteorological Institute Rep. 16/2010, 7 pp.

——, Ø. Saetra, T. Lien, and Y. Gusdal, 2011: A climatological study of polar lows in the Nordic Seas. *Quart. J. Roy. Meteor. Soc.*, **137**, 1762–1772, doi:10.1002/qj.846.

Rasmussen, E., and J. Turner, 2003: *Polar Lows: Mesoscale Weather Systems in the Polar Regions*. Cambridge University Press, 612 pp.

Sardeshmukh, P. D., and B. I. Hoskins, 1984: Spatial smoothing on the sphere. *Mon. Wea. Rev.*, **112**, 2524–2529, doi:10.1175/1520-0493(1984)112<2524:SSOTS>2.0.CO;2.

Smirnova, J. E., P. A. Golubkin, L. P. Bobylev, E. V. Zabolotskikh, and B. Chapron, 2015: Polar low climatology over the Nordic and Barents Seas based on satellite passive microwave data. *Geophys. Res. Lett.*, **42**, 5603–5609, doi:10.1002/2015GL063865.

Terpstra, A., C. Michel, and T. Spengler, 2016: Forward and reverse shear environments during polar low genesis over the northeast Atlantic. *Mon. Wea. Rev.*, **144**, 1341–1354, doi:10.1175/MWR-D-15-0314.1.

Tilinina, N., S. K. Gulev, and D. H. Bromwich, 2014: New view of Arctic cyclone activity from the Arctic system reanalysis. *Geophys. Res. Lett.*, **41**, 1766–1772, doi:10.1002/2013GL058924.

Wentz, F. J., 1997: A well-calibrated ocean algorithm for special sensor microwave/imager. *J. Geophys. Res.*, **102**, 8703–8718, doi:10.1029/96JC01751.

Wilhelmsen, K., 1985: Climatological study of gale-producing polar lows near Norway. *Tellus*, **37A**, 451–459, doi:10.1111/j.1600-0870.1985.tb00443.x.

Yanase, W., H. Niino, S. I. I. Watanabe, K. Hodges, M. Zahn, T. Spengler, and I. A. Gurvich, 2016: Climatology of polar lows over the Sea of Japan using the JRA-55 reanalysis. *J. Climate*, **29**, 419–437, doi:10.1175/JCLI-D-15-0291.1.

Zahn, M., and H. von Storch, 2008: A long-term climatology of North Atlantic polar lows. *Geophys. Res. Lett.*, **35**, L22702, doi:10.1029/2008GL035769.

Zappa, G., L. Shaffrey, and K. Hodges, 2014: Can polar lows be objectively identified and tracked in the ECMWF operational analysis and the ERA-Interim reanalysis? *Mon. Wea. Rev.*, **142**, 2596–2608, doi:10.1175/MWR-D-14-00064.1.